

mosphere. The graphite cathode of 10 mm diameter was placed horizontally facing the composite anode of 6.15 mm diameter. The latter had a 3.2 mm diameter hole drilled 25 mm filled with a mixture of graphite (Graphit, fein gepulvert reinst, Merck, Germany) and Si powder in the atomic ratio 1:1.

The experiments were repeated with and without the addition of 0.03 at.-% of Fe powder to the anode. During arc-discharge evaporation of the graphite/silicon composite anode a hard cylindrical deposit (the core deposit) grows at the end of the graphitic cathode. Additionally a soot-like deposit is formed around the core deposit of the cathode, here called the collaret deposit. Samples for TEM examination were prepared from the core deposit as well as from the collaret deposit. The deposits were diluted in chloroform, sonicated for 5 min and dropped on a TEM Cu grid (300 mesh) with holey carbon film.

The characterization of the samples was performed using TEM, HRTEM, electron diffraction, and analytical electron microscopy using EELS.

TEM was carried out with a JEM 2000FX (JEOL, Japan), using an acceleration voltage of 200 kV, HRTEM was carried out with a JEM 4000EX (JEOL, Japan), using an acceleration voltage of 400 kV, and EELS was carried out with a PEELS 666 (Gatan, USA) on a dedicated STEM VG HB 501 UX (Vacuum Generators, UK) operating with a cold field emission gun at 100 kV acceleration voltage. All EELS data were acquired and processed using the EL/P 3.0 software (Gatan, USA). Pure Si and SiC powder samples prepared for electron microscopy in the same way as the arc discharge products were characterized by EELS in order to get reference spectra acquired under comparable conditions.

The Si-L edges were acquired with an energy dispersion of 0.1 eV, a convergence angle of 10 mrad and a collector angle of 6.5 mrad. For the measurement of the Si-K edge the gun-lens was less excited to get a sufficient electron intensity at energy losses of about 1800 eV; the energy dispersion was adjusted at 1.0 eV. The Si-K edges were measured with a convergence angle of 10 mrad and a collector angle of 13 mrad.

The energy location of the Si-L and the C-K edges was calibrated using zero-loss spectra acquired before the measurements. As a result the error of the energy location is less than  $\pm 0.2$  eV. A deconvolution of the low-loss spectra was performed to remove the effect of sample thickness on the ELNES of the spectra.

Received: February 22, 1999  
Final version: November 3, 1999

- [1] L. E. Brus, R. W. Siegel, R. P. Andres, R. S. Averbeck, W. L. Brown, W. A. Goddard, A. Kaldor, S. G. Louie, M. Moscovits, P. S. Peercy, S. J. Riley, F. Spaepen, Y. Wang, *J. Mater. Res.* **1989**, *4*, 704.
- [2] L. T. Canham, *Appl. Phys. Lett.* **1990**, *57*, 1046.
- [3] G. G. Quin, Y. Q. Jia, *Solid State Commun.* **1993**, *86*, 559.
- [4] W. L. Wilson, P. F. Szajowski, L. E. Brus, *Science* **1993**, *262*, 1242.
- [5] Z. Zhang, *Microsc. Res. Tech.* **1998**, *40*, 163.
- [6] *Gmelin Handbook of Inorganic Chemistry, Silicon Suppl.*, 8th ed., Springer, Berlin **1986**, Vol. B3, p. 507.
- [7] *Diamond, SiC and Nitride Wide Bandgap Semiconductors* (Eds: C. H. Carter, G. Gildenblat, S. Nakamura), Symp. Mater. Res. Soc., MRS, Pittsburgh, PA **1994**.
- [8] W. R. Cannon, S. C. Danforth, J. S. Haggarty, R. A. Marra, *J. Am. Ceram. Soc.* **1982**, *65*, 330.
- [9] C. M. Hollabaugh, D. E. Hull, L. Newkirk, J. J. Petrovic, *J. Mater. Sci.* **1983**, *18*, 3190.
- [10] Y. Suama, R. M. Marra, J. S. Haggarty, H. K. Bowen, *Am. Ceram. Soc. Bull.* **1985**, *64*, 1356.
- [11] H. Dai, E. W. Wong, Y. Z. Lu, S. Fan, C. Lieber, *Nature* **1995**, *375*, 769.
- [12] G. W. Meng, L. D. Zhang, C. M. Mo, S. J. Zhang, Y. Quing, S. P. Feng, H. J. Li, *Solid State Commun.* **1998**, *106*, 215.
- [13] Y. Zhang, K. Suenaga, C. Colliex, S. Iijima, *Science* **1998**, *281*, 973.
- [14] H. Funasaka, K. Sugiyama, K. Yamamoto, T. Takahashi, *J. Appl. Phys.* **1995**, *78*, 5320.
- [15] J. Jiao, S. Seraphin, X. Wang, J. C. Withers, *J. Appl. Phys.* **1996**, *80*, 103.
- [16] S. Seraphin, D. Zhou, J. Jiao, *J. Appl. Phys.* **1996**, *80*, 2097.
- [17] Y. Saito, K. Nishikubo, K. Kawabata, T. Matsumoto, *J. Appl. Phys.* **1996**, *80*, 5320.
- [18] Y. Saito, T. Matsumoto, K. Nishikubo, *J. Cryst. Growth* **1997**, *172*, 163.
- [19] R. F. Egerton, *Electron Energy Loss Spectroscopy in the Electron Microscope* Plenum, New York **1996**, p. 201.
- [20] R. F. Egerton, *Electron Energy Loss Spectroscopy in the Electron Microscope* Plenum, New York **1996**, p. 225.
- [21] M. Altarelli, D. L. Dexter, *Phys. Rev. Lett.* **1972**, *29*, 1100.
- [22] R. Schneider, J. Woltersdorf, O. Lichtenberger, *J. Microsc.* **1996**, *183*, 39.
- [23] R. S. Wagner, W. C. Ellis, *Trans. Met. Soc. AIME* **1965**, *233*, 1053.
- [24] G. A. Bootsma, W. F. Knippenberg, G. Verspui, *J. Cryst. Growth* **1971**, *11*, 297.

- [25] G. Urretavizcaya, J. M. Porto López, *J. Mater. Res.* **1994**, *9*, 2981.
- [26] F. J. Narisco-Romero, F. Rodríguez-Reinoso, *J. Mater. Sci.* **1996**, *31*, 779.
- [27] T. Belmonte, L. Bonnetain, J. L. Ginoux, *J. Mater. Sci.* **1996**, *31*, 2367.
- [28] T. B. Massalski, *Binary Alloy Phase Diagrams* ASM International, Materials Park, OH **1990**, Vol. 2, p. 1772.
- [29] C. J. Smithells, *Metals Reference Book* Butterworths, London **1967**, Vol. 1, p. 262.

## Gain Effects in Optical Storage: Thermal Induction of a Surface Relief Grating in a Smectic Liquid Crystal\*\*

By Andreas Stracke, Joachim H. Wendorff,\*  
Daniela Goldmann, Dietmar Janietz, and Burkard Stiller

Optical storage processes based on light-induced isomerization cycles in low molar mass and polymeric organic materials containing azobenzene groups are well-documented in the literature.<sup>[1–9]</sup> Linearly polarized light causes a photoinduced reorientation process of molecular groups even within the solid glassy state and thus gives rise to strong optical effects. Reversible digital and holographic storage have been demonstrated for amorphous and liquid-crystalline films. Amorphous materials have the advantage that optically homogeneous non-scattering films can be manufactured easily by spin coating from solution, whereas liquid-crystalline materials require the induction of monodomains. This can be achieved by the presence of external fields or of pretreated surfaces of the substrate. Liquid-crystalline materials, on the other hand, have the tendency to display stronger optical effects due to the presence of highly ordered domains.

More recently it was shown that the two approaches can be combined.<sup>[10–14]</sup> The concept consists of disturbing the liquid-crystalline phase formation in such a way that it can be suppressed. Relevant examples are rapid manufacturing processes such as spin-coating of thin films. Amorphous homogeneous films result, or films with liquid-crystalline domains that are too small to be detectable and to give rise to scattering. Such films display the highly interesting property of a gain effect in holographic optical storage. A holographic grating is written-in by the superposition of two intersecting light beams in the plane of the recording film. The sinusoidal intensity modulation gives rise to a corresponding modulation of the optical properties: the refractive index or birefringence. These modulations can be read out with a sec-

[\*] Dr. J. H. Wendorff, Dr. A. Stracke  
Institut für Physikalische Chemie und  
Wissenschaftliches Zentrum für Materialwissenschaften  
Philipps-Universität Marburg  
Hans-Meerwein-Strasse, D-35032 Marburg (Germany)  
Dr. D. Goldmann, Dr. D. Janietz, Dr. B. Stiller  
Fachbereich Chemie und Institut für Dünnschichttechnologie  
Universität Potsdam  
Am Neuen Palais 10, D-14469 Potsdam (Germany)

[\*\*] We gratefully acknowledge the financial support of the Deutsche Forschungsgemeinschaft (Ja 668/6-1 and We 496/14-1) and the Fonds der Chemischen Industrie.

ond light beam yielding the diffraction efficiency as a measure of the magnitude of the induced modulations. The diffraction efficiency  $\eta$  is defined as  $\eta = I/I_0$ , where  $I$  and  $I_0$  are the intensity scattered along the first scattering maximum, and the primary beam intensity, respectively.

It is observed that the efficiency may be rather limited if the holographic grating is stored in the amorphous film. Yet it increases strongly, even in the absence of the writing beams, if the film is annealed within a temperature range above the glass transition temperature and below the clearing temperature of the liquid-crystalline phase. Gain factors,  $g$ , defined as the ratio of the diffraction efficiency after and before the annealing, of more than 10 have been reported in the literature.<sup>[15]</sup> Such gain effects have been found for calamitic systems, that is for systems containing rod-like mesogenic units, and also for more complex systems containing both rod-like and disc-like units.<sup>[16]</sup> The gain effect has been attributed to liquid-crystalline self-organization processes taking place during annealing. The orientation of the resulting domains is controlled by the photoinduced orientation taking place during the writing process in the amorphous state. The strongest gain effect that can be achieved in this way is thus controlled by the perfection of the reorientation process and the intrinsic orientational order within the liquid-crystalline domains.

More recently it was found that the light-induced isomerization of azobenzene units does in certain cases not only give rise to photo-reorientation but may also cause surface modulations. A periodic surface relief grating pattern (SRG) may result in the case of grating experiments.<sup>[17–20]</sup> This effect has been attributed to the formation of additional free volume by the isomerization process and the resulting pressure gradients. The formation of such a relief pattern has been found to depend on parameters such as the state of polarization of the intersecting beams, the molecular weight and molecular weight distribution of the materials used for storage. In any case the surface pattern constitutes a storage process since it gives rise to the diffraction of the reading beams.

In this contribution we describe our efforts to exploit a combination of photo-orientation and the formation of a surface relief pattern to enhance the gain effect even further. Such an enhancement is of considerable technical importance. It allows strong optical modulations to be induced, the sensitivity of the material to be increased, and the energy required for the storage process to be reduced.

We decided to select a low molar mass smectic system since, in the light of the theoretical approaches,<sup>[21]</sup> such a system should have a strong tendency to form the surface pattern but should also display strong photoreorientation effects. We selected a material that can be quenched into an amorphous state despite the low molar mass.

The investigated liquid-crystalline model compound tris-azomelamine (TAM) consists of a triazine core, linked with three rod-like azobenzene units bearing a  $C_{12}$ -alkyl chain

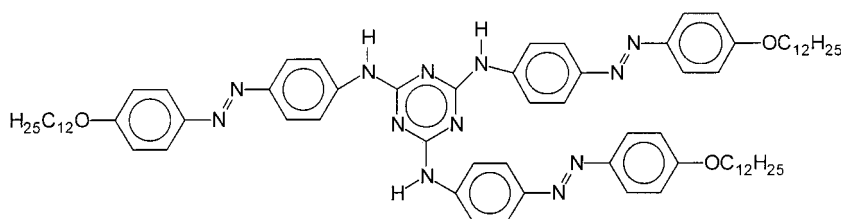


Fig. 1. Chemical structure of the smectic trisazomelamine TAM.

(Figure 1). The synthesis and a detailed characterization of the mesophase behavior of TAM and a number of homologues have been reported previously.<sup>[22]</sup>

The compound is isotropic above 239 °C and a nematic phase is observed on cooling, which changes to a smectic phase below 221 °C. By rapid cooling, the Sm-phase can be frozen into the glassy state ( $T_g = 32$  °C). Amorphous, optically transparent films can be obtained from a chloroform solution by the spin-coating technique. These films (with a thickness of 0.4–2  $\mu\text{m}$ ) show no significant birefringence up to 109 °C on heating, indicating that the liquid-crystalline phase is kinetically suppressed up to this temperature.

The writing beam propagates in the  $z$ -direction and is  $y$ -polarized (s-polarization). We used s-polarized writing beams to minimize the effect of SRG formation during the writing process at room temperature, since it is known that s-polarized beams induce only weak or even no surface gratings, at least in polymers.<sup>[17,23]</sup> The set-up of the holographic grating experiment is described in more detail in the experimental part.

When irradiated with linearly polarized light a stable optical grating can be induced in an amorphous film of TAM, as apparent from Figure 2, which displays the increase of the diffraction efficiency of the amorphous film as a function of the irradiation time. Diffraction efficiencies of up to

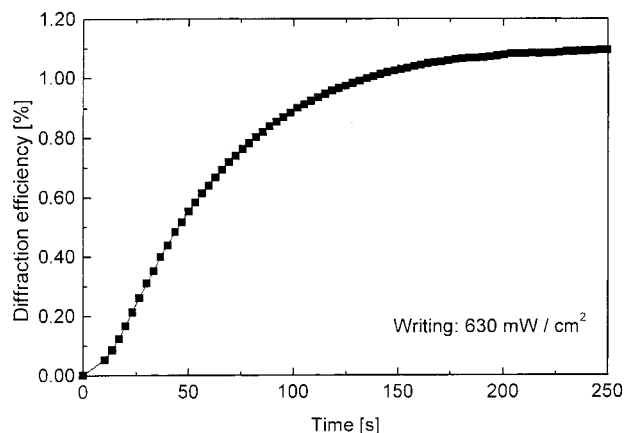


Fig. 2. Holographic growth curve.

about 5 % (which corresponds to a photoinduced birefringence of  $\Delta n = 0.18$ ) can be achieved in this way for thin gratings. We will concentrate in the following on gratings characterized by diffraction efficiencies of the order of 1 %. The grating remains stable if the writing beams are

shut off: no significant back relaxation of the signal is observed at room temperature during the first hours after the end of the writing process.

The  $\Delta n$  values calculated from the diffraction efficiencies agree with those of birefringence measurements within the limits of experimental error. This indicates that the grating results predominantly from the bulk effect, that is, the re-orientation of molecular axes. In fact, the surface of the film is to a first approximation flat.

The efficiency of the photoinduced grating can be raised significantly without any additional irradiation by heating the sample above the glass transition (Fig. 3).

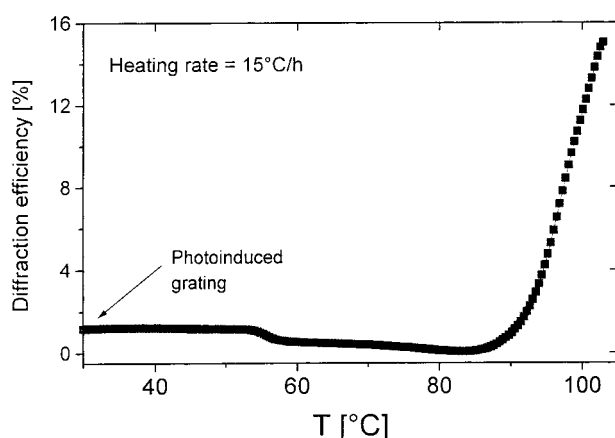


Fig. 3. Thermal development of a photoinduced grating (heating rate 15 °C/h).

The enhancement of the grating's efficiency can be quantified by defining a gain coefficient,  $g$ .<sup>[15]</sup>

$$g = \frac{\eta_{\max}}{\eta_{\text{wrt}}} \quad (1)$$

where the indices "wrt" and "max" indicate the efficiencies at the end of the writing process and at the maximum of the diffraction obtained during the thermal treatment, respectively.

Figure 3 displays the increase in the diffraction efficiency due to the thermal treatment. The experiments reveal that the gain process depends on the heating rate. A maximum value of  $\eta$  of up to 20 % can be achieved by using a slow heating rate (<20 °C/h). This corresponds to a refractive index change of 0.25.<sup>[24,25]</sup> For these conditions gain factors of about  $g = 30$  can be obtained, if the photoinduced grating is below the level of optical saturation. The gain effect may be explained in terms of a thermally induced reorientation process of the mesogenic chromophores leading to a higher birefringence.<sup>[13,15]</sup> On the other hand, it is known that the formation of sinusoidal surface modulations will result in high diffraction efficiencies far above the saturation level of the refractive index grating.<sup>[17,25]</sup> Indeed, the experiments show the formation of a surface relief pattern due to the thermal treatment. Figure 4 displays a comparison of a weak photoinduced SRG profile and the same grating after the annealing process described above. After the thermal treatment the modulation depth of the grating is found to

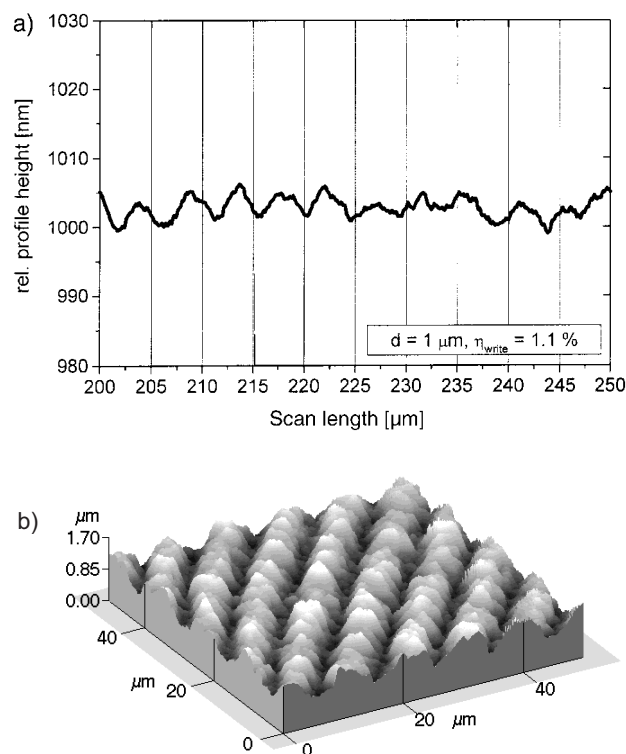


Fig. 4. a) Surface profile of the photoinduced grating with only weak surface modulations (<5 nm), b) AFM image of the irradiated area after thermal treatment.

be larger than 400 nm as compared to less than 5 nm prior to annealing.

The experiment thus gives evidence that the gain effect is not only caused by a reorientational (bulk) process but is also due to migration processes (surface modulation). However, up to now we have not succeeded in separating both contributions to the overall efficiency, yet further studies are in progress.

We have thus demonstrated that the strong amplification of the contrast of photoinduced gratings by a thermal development of the liquid-crystalline samples prepared in the amorphous state is not only due to an enhancement of photo-orientation in the liquid-crystalline phase. It is also a consequence of the formation of surface relief patterns and their amplification during the thermal treatment. The effect takes place above the glass transition and seems to be controlled by the suppression of the thermotropic phase formation in the glassy state on the one hand and the tendency of mesogenic self-organization at elevated temperatures due to the liquid-crystalline potential on the other hand.

The combination of photo-orientation and surface formation might be used for the development of highly efficient storage materials and optical devices based on liquid-crystalline azo compounds. In a first step, the information can be written-in optically with low laser exposure and in a second step the contrast can be amplified significantly by thermal development within the mesophase.

## Experimental

The set-up of the holographic grating experiment is sketched in Figure 5. Intensity gratings with a grating constant of  $\Lambda = 5.1 \mu\text{m}$  were obtained by the interference of two coherent, linearly polarized laser beams in the plane of the sample. We used a continuous wave argon ion laser operating at

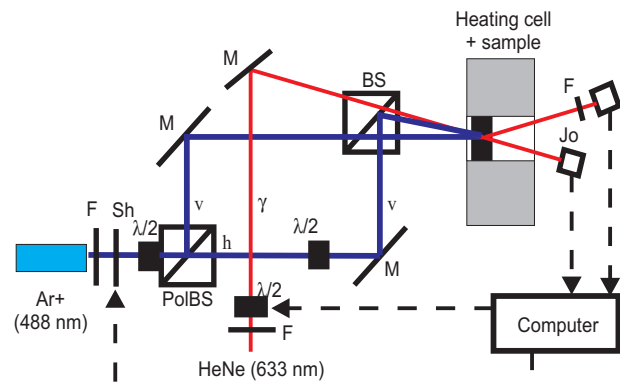


Fig. 5. Set-up of the holographic grating experiment (F = filter; Sh = shutter; BS = beam splitter, PolBS = polarizing beam splitter; M = mirror;  $\lambda/2$  = half wave plate;  $D_0$ ,  $D_1$  = detector; the letters v and h denote the vertical and horizontal polarization directions of the writing beam, respectively). The polarization direction of the reading beam can be rotated by an angle  $\gamma$  with respect to the vertical orientation. (The origin of the small change in the diffraction efficiency at about  $55^\circ\text{C}$  is rather complex and is discussed in a separate paper [25].)

488 nm and we used laser intensities in the range  $30\text{--}1600 \text{ mW/cm}^2$  for the writing of the gratings. In this range we found no dependence of the holographic growth characteristics on the intensity. The resulting refractive index modulation

$$n(x) = n_0 + n_1 \cos\left(\frac{2\pi x}{\Lambda}\right) \quad (2)$$

was read out via the diffraction of a HeNe laser beam at 633 nm. The experimentally obtained diffraction efficiency is proportional to the square sine of the induced refractive index change  $n_1$ , which in turn is related to the induced orientational order of the optical axes of the azo dyes.

Using the  $Q$ -parameter, defined as follows:

$$Q = \frac{2\pi\lambda_{\text{HeNe}}d}{n_0\Lambda^2} \quad (3)$$

( $d$  = sample thickness,  $n_0$  = refractive index of the material, and  $\Lambda$  = grating constant) as a criterion for the classification of thin and thick gratings ( $0 < Q < 1$  = thin gratings;  $Q \geq 10$  = thick gratings;  $1 \leq Q < 10$  = intermediate region) we find that all investigated film samples have  $Q$ -parameters  $< 1$  and thus are thin gratings. For the calculation of the refractive index changes from the measured diffraction efficiencies we thus used an approximation of the Bessel functions for thin gratings [26].

$$2n_1 \approx \frac{\lambda_c}{\pi d} 1.171 \arcsin(1.7185\sqrt{\eta}) \quad (4)$$

We employed a polarizing beam splitter and half-wave plates in order to achieve equal polarization directions for the writing and the reading beams, as well as two writing beams of equal intensity.

The surface profile measurements were performed with a Dektak profile analyzer (Dektak3ST, Veeco) and an Atomic force microscope (AFM, SA 1/BD 2, Park-Scientific Instruments).

Received: September 6, 1999  
Final version: November 19, 1999

[1] M. Eich, J. H. Wendorff, B. Reck, H. Ringsdorf, *Makromol. Chem. Rapid Commun.* **1987**, 8, 59.

[2] S. Ovanov, I. Yakolev, S. Kostromine, V. Shibaev, V. L. Laessker, J. Stumpe, D. Kreyssig, *Makromol. Chem. Rapid Commun.* **1991**, 12, 709.

- [3] A. Petri, S. Kummer, C. Braeuchle, *Liq. Cryst.* **1995**, 19, 277.  
[4] K. Anderle, R. Birenheide, M. Eich, J. H. Wendorff, *Makromol. Chem. Rapid Commun.* **1989**, 10, 477.  
[5] M. Eich, J. H. Wendorff, *J. Opt. Soc. Am.* **1990**, B7, 1428.  
[6] K. Anderle, J. H. Wendorff, *Mol. Cryst. Liq. Cryst.* **1994**, 243, 51.  
[7] M. Ivanov, T. Todrov, L. Nikolova, N. Tomova, V. Dragostinova, *Appl. Phys. Lett.* **1995**, 66, 2174.  
[8] R. Birenheide, J. H. Wendorff, *SPIE Proc.* **1990**, 1213.  
[9] T. Fuhrmann, M. Kunze, J. H. Wendorff, *Makromol. Theory Simul.* **1998**, 7, 421.  
[10] L. Laesker, T. Fischer, J. Stumpe, S. Kostromine, S. Ivanov, V. Shibaev, R. Ruhmann, *Mol. Cryst. Liq. Cryst.* **1994**, 253, 1.  
[11] T. Bieringer, R. Wuttke, D. Haarer, *Macromol. Chem Phys.* **1995**, 196, 1375.  
[12] A. Natansohn, P. Rochon, M. Pézolet, P. Audet, D. Brown, S. To, *Macromolecules* **1994**, 27, 2580.  
[13] S. J. Zilker, T. Bieringer, D. Haarer, R. S. Stein, J. W. van Egmond, *Adv. Mater.* **1998**, 10, 855.  
[14] Th. Fuhrmann, M. Hosse, I. Lieker, J. Rübner, A. Stracke, J. H. Wendorff, *Liq. Cryst.* **1999**, 26, 779.  
[15] T. Bieringer, PhD Thesis, Bayreuth **1996**.  
[16] A. Stracke, J. H. Wendorff, D. Janietz, S. Mahlstedt, *Adv. Mater.* **1999**, 11, 667.  
[17] D. Y. Kim, L. Li, X. L. Jiang, V. Shivshankar, J. Kumar, S. K. Tripathy, *Macromolecules* **1995**, 28, 8835.  
[18] P. Rochon, E. Batalla, A. Natansohn, *Appl. Phys. Lett.* **1995**, 66, 136.  
[19] P. Lefin, C. Fiorini, J. M. Nunzi, *Pure Appl. Opt.* **1998**, 7, 71.  
[20] T. G. Pedersen, P. M. Johansen, N. C. R. Holme, P. S. Ramanujam, S. Hvilsted, *Phys. Rev. Lett.* **1998**, 80, 89.  
[21] C. J. Barrett, P. L. Rochon, A. Natansohn, *J. Chem. Phys.* **1998**, 109, 1505.  
[22] D. Goldmann, D. Janietz, C. Schmidt, J. H. Wendorff, *Liq. Cryst.* **1998**, 25, 711.  
[23] N. C. R. Holme, L. Nikolova, P. S. Ramanujam, S. Hvilsted, *Appl. Phys. Lett.* **1997**, 70, 1518.  
[24] A. Stracke, PhD Thesis, Marburg **1999**.  
[25] A. Stracke, J. H. Wendorff, D. Goldmann, D. Janietz, B. Stiller, unpublished.  
[26] C. J. Barrett, A. L. Natansohn, P. L. Rochon, *J. Phys. Chem.*, **1996**, 100, 8836.

## Fabrication of a Sexithiophene Semiconducting Wire: Nanoshaving with an Atomic Force Microscope Tip\*\*

By Anna B. Chwang, Eric L. Granstrom, and  
C. Daniel Frisbie\*

Recent advances in organic-based electronics highlight the potential utility of devices employing organic semiconductors.<sup>[1]</sup> Also of considerable interest are methods by which these materials can be deposited and patterned. Vacuum sublimation and spin-coating are widely used for the deposition of organic semiconductor films, and patterning by soft lithography, photolithography, and printing techniques has been demonstrated.<sup>[2]</sup> In previous studies we have used vacuum sublimation as a reliable method for depositing individual grains of the organic semiconductor sexithiophene

[\*] Dr. C. D. Frisbie, A. B. Chwang, Dr. E. L. Granstrom  
Department of Chemical Engineering and Materials Science  
University of Minnesota  
421 Washington Avenue SE, Minneapolis, MN 55455 (USA)

[\*\*] This work was supported by the David and Lucile Packard Foundation and by the National Science Foundation under DMR-9624154-001. ELG acknowledges support from the National Defense Science and Engineering Graduate Fellowship program.